JCI The Journal of Clinical Investigation

Ube3a reinstatement mitigates epileptogenesis in Angelman syndrome model mice

Bin Gu, … , Serena M. Dudek, Benjamin D. Philpot

J Clin Invest. 2019;129(1):163-168. https://doi.org/10.1172/JCI120816.

Concise Communication **Neuroscience**

Angelman syndrome (AS) is a neurodevelopmental disorder in which epilepsy is common (~90%) and often refractory to antiepileptics. AS is caused by mutation of the maternal allele encoding the ubiquitin protein ligase E3A (UBE3A), but it is unclear how this genetic insult confers vulnerability to seizure development and progression (i.e., epileptogenesis). Here, we implemented the flurothyl kindling and retest paradigm in AS model mice to assess epileptogenesis and to gain mechanistic insights owed to loss of maternal *Ube3a*. AS model mice kindled similarly to wild-type mice, but they displayed a markedly increased sensitivity to flurothyl-, kainic acid–, and hyperthermia-induced seizures measured a month later during retest. Pathological characterization revealed enhanced deposition of perineuronal nets in the dentate gyrus of the hippocampus of AS mice in the absence of overt neuronal loss or mossy fiber sprouting. This pro-epileptogenic phenotype resulted from *Ube3a* deletion in GABAergic but not glutamatergic neurons, and it was rescued by pancellular reinstatement of *Ube3a* at postnatal day 21 (P21), but not during adulthood. Our results suggest that epileptogenic susceptibility in AS patients is a consequence of the dysfunctional development of GABAergic circuits, which may be amenable to therapies leveraging juvenile reinstatement of *UBE3A*.

Ube3a reinstatement mitigates epileptogenesis in Angelman syndrome model mice

Bin Gu,[1] Kelly E. Carstens,[1,2] Matthew C. Judson,[1,3] Katherine A. Dalton,[4] Marie Rougié,[1] Ellen P. Clark,[1] Serena M. Dudek,[2] and Benjamin D. Philpot[1,3,5]

[1]Department of Cell Biology and Physiology, University of North Carolina, Chapel Hill, North Carolina, USA. [2]Neurobiology Laboratory, National Institute of Environmental Health Sciences, NIH, Research Triangle Park, North Carolina, USA. [3]Carolina Institute for Developmental Disabilities, [4]Psychology and Neuroscience Program, and [5]UNC Neuroscience Center, University of North Carolina, Chapel Hill, North Carolina, USA.

Angelman syndrome (AS) is a neurodevelopmental disorder in which epilepsy is common (~90%) and often refractory to antiepileptics. AS is caused by mutation of the maternal allele encoding the ubiquitin protein ligase E3A (UBE3A), but it is unclear how this genetic insult confers vulnerability to seizure development and progression (i.e., epileptogenesis). Here, we implemented the flurothyl kindling and retest paradigm in AS model mice to assess epileptogenesis and to gain mechanistic insights owed to loss of maternal *Ube3a*. AS model mice kindled similarly to wild-type mice, but they displayed a markedly increased sensitivity to flurothyl-, kainic acid–, and hyperthermia-induced seizures measured a month later during retest. Pathological characterization revealed enhanced deposition of perineuronal nets in the dentate gyrus of the hippocampus of AS mice in the absence of overt neuronal loss or mossy fiber sprouting. This pro-epileptogenic phenotype resulted from *Ube3a* deletion in GABAergic but not glutamatergic neurons, and it was rescued by pancellular reinstatement of *Ube3a* at postnatal day 21 (P21), but not during adulthood. Our results suggest that epileptogenic susceptibility in AS patients is a consequence of the dysfunctional development of GABAergic circuits, which may be amenable to therapies leveraging juvenile reinstatement of *UBE3A*.

Introduction

Deletions or mutations of the maternally inherited copy of the *UBE3A* gene cause Angelman syndrome (AS). Individuals with AS exhibit developmental delay, motor dysfunction, lack of speech, and highly penetrant EEG abnormalities and seizures (1, 2). Epilepsy in AS is common (80%–95% penetrance), polymorphic, and often resistant to available antiepileptic drugs. The frequency, severity, and pharmacological intractability of the seizures exact a heavy toll on the quality of life of individuals with AS and their caregivers (1–6). AS model mice lacking a functional maternal copy of the orthologous *Ube3a* gene (*Ube3a*$^{m-/p+}$) exhibit many clinical aspects of AS, including EEG abnormalities and circuit hyperexcitability, and offer a preclinical model for developing new therapeutics (7–13). To date, studies of epilepsy in AS model mice have utilized acute seizure induction paradigms, which illuminate mechanisms of ictogenesis but fail to provide insight into how seizures develop and progress over time (7–12). This paucity of knowledge regarding epileptogenic mechanisms in AS is a barrier to the development of effective therapies.

Although there is currently no cure for AS, *UBE3A* gene replacement or reactivation of the inactive, epigenetically silenced paternal *UBE3A* allele in neurons holds great therapeutic promise, including for the treatment of epilepsy (14–17). However, many AS phenotypes in mouse models are impervious to rescue by reinstatement of *Ube3a* beyond the early stages of postnatal development (11), suggesting that there is a critical period for therapeutic recovery. Determining whether epileptogenesis is similarly refractory to later postnatal and adult *UBE3A* reinstatement, and identifying the neural circuits through which *UBE3A* reexpression mediates its antiepileptogenic effects, will be necessary to guide the optimal implementation of emerging *UBE3A*-reinstatement therapies. These efforts also promise to help refine existing strategies to treat intractable epilepsy in AS and perhaps other neurodevelopmental disorders.

Results and Discussion

Flurothyl kindling (flurothyl exposure once daily for 8 days, and retest at day 36) allows for the assessment of both ictogenic and epileptogenic properties in mice (Figure 1A and refs. 18, 19). We tested adult AS model mice (*Ube3a*$^{m-/p+}$) in this paradigm, finding that they exhibited similar seizure susceptibility in response to an initial flurothyl exposure (day 1), but kindled somewhat more slowly than wild-type (WT) controls during the induction phase (Figure 1, B and C, and Supplemental Table 1; supplemental material available online with this article; https://doi.org/10.1172/JCI120816DS1). This indicated that adult naive AS mice (on C57BL/6J background) have a relatively normal response to flurothyl, consistent with previous studies utilizing other convulsive stimuli (7–10). However, upon being retested with flurothyl following a month-long incubation period without exposure to

Conflict of interest: The authors have declared that no conflict of interest exists.

Submitted: March 1, 2018; **Accepted:** October 11, 2018.
Reference information: *J Clin Invest*. 2019;129(1):163–168.
https://doi.org/10.1172/JCI120816.

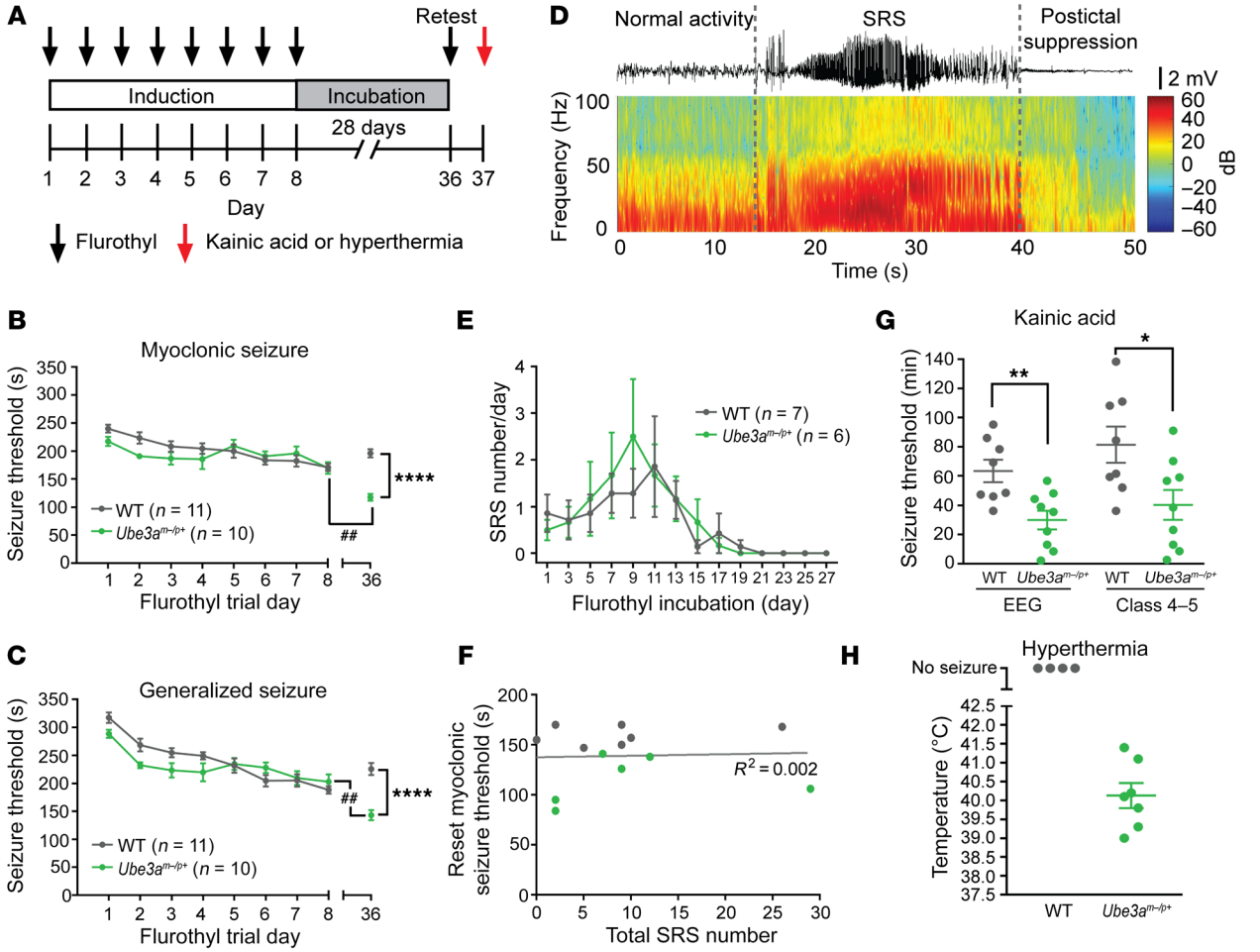

Figure 1. AS mice exhibit exaggerated epileptogenesis. (**A**) Experimental paradigm of flurothyl kindling and retest followed by kainic acid–induced (repeated low-dose injection of 5 mg/kg i.p. every 30 minutes) or hyperthermia-induced seizure. Latency to (**B**) myoclonic and (**C**) generalized seizure in WT and AS model mice during flurothyl kindling and retest. $^{\#\#}P < 0.01$ compared with day 8 of AS model mice; $^{****}P < 0.0001$ compared with WT; 2-way ANOVA with Bonferroni's post hoc test. (**D**) Representative EEG trace of a spontaneous recurrent seizure (SRS) with corresponding spectrogram recorded from a WT mouse during the incubation period. (**E**) Group analysis of SRS incidence, recorded every other day during the 28-day incubation period following flurothyl kindling. (**F**) Correlation for individual WT (gray) and AS (green) mice between SRS frequency during incubation period and myoclonic seizure threshold at flurothyl retest. (**G**) Latency to the onset of repeated low-dose injection of kainic acid–induced EEG and class 4 to 5 behavioral seizure in kindled WT ($n = 8$) and AS ($n = 9$) model mice. $^{*}P < 0.05$, $^{**}P < 0.01$ by unpaired t test. (**H**) Hyperthermia-induced seizure incidence and body temperature at which generalized seizure occurred in kindled WT ($n = 4$) and AS ($n = 7$) model mice.

the drug (day 36), AS mice showed a striking reduction in seizure threshold, not only in comparison with WT, but also in comparison with their own day 8 responses at the completion of flurothyl kindling (Figure 1, B and C).

Given that spontaneous recurrent seizures (SRSs) manifest and rapidly evolve in C57BL/6J mice following 8-day kindling with flurothyl (18), we hypothesized that SRSs in AS mice might occur more frequently or with altered temporal dynamics during the month-long incubation period, possibly explaining the exaggerated seizure phenotype that we observed upon retest (20). We therefore monitored SRSs during the incubation period by chronic video-EEG recording in a separate cohort of flurothyl-kindled WT and AS model mice. We found both the frequency and temporal evolution of SRSs to be similar between groups (Figure 1, D and E), indicating that exaggerated epileptogenesis in flurothyl-kindled AS mice is not due to the differential expression of SRSs (Figure 1F).

Does the pro-epileptogenic phenotype precipitated by flurothyl kindling generalize across circuits and to other models of seizure induction? We first addressed this question by measuring the response of flurothyl-kindled AS and WT mice to repeated systemic administration of kainic acid (21), which predominantly triggers limbic seizures (22). Kainic acid evoked more severe electrographic and behavioral seizure responses in flurothyl-kindled AS mice compared with WT (Figure 1G). Because AS individuals tend to have seizures during febrile episodes or even following moderate increases in body temperature (4, 5), we also challenged kindled WT and AS with hyperthermia, by slowly raising body temperature in a carefully controlled fashion to 42.5°C. No WT mice seized in this paradigm, whereas all AS model mice exhibited generalized seizures at a modestly elevated (average = 40.1°C) body temperature (Figure 1H).

We previously found that GABAergic, but not glutamatergic, neuron–specific loss of *Ube3a* causes hyperexcitability within

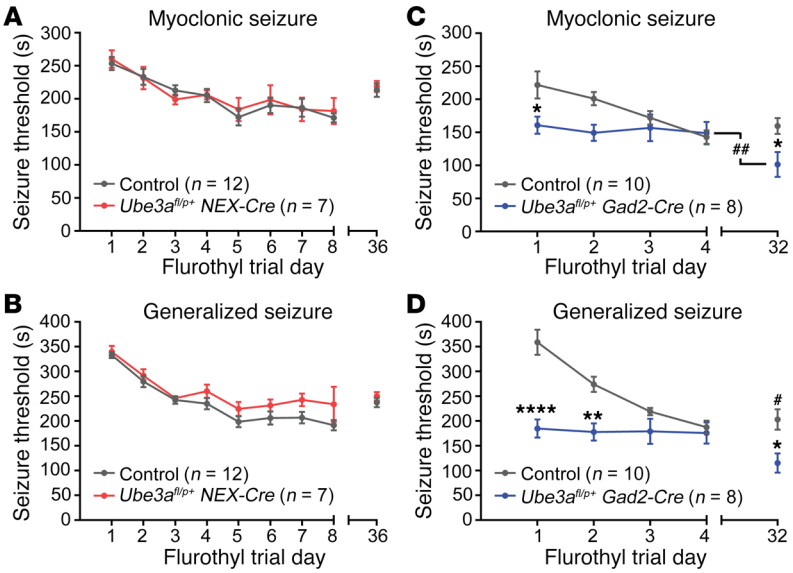

Figure 2. GABAergic neuron–specific loss of *Ube3a* enhances epileptogenesis. (**A** and **B**) Latency to myoclonic (**A**) and generalized (**B**) seizures during 8-day flurothyl kindling and retest in control mice or mice with glutamatergic neuron–specific loss of *Ube3a* (*Ube3a*$^{fl/p+}$ *NEX-Cre*). (**C** and **D**) Latency to myoclonic (**C**) and generalized (**D**) seizures during 4-day flurothyl kindling and retest in control mice or mice with GABAergic neuron–specific loss of *Ube3a* (*Ube3a*$^{fl/p+}$ *Gad2-Cre*). $^{\#}P < 0.05$ compared with day 1 of control; $^{\#\#}P < 0.01$ compared with day 4 of *Ube3a*$^{fl/p+}$ *Gad2-Cre* mice; $^{*}P < 0.05$, $^{**}P < 0.01$, $^{****}P < 0.0001$ compared with control; 2-way ANOVA with Bonferroni's post hoc test.

the neocortex and in broader behavioral contexts in mice (12). Accordingly, we explored the neuron type–specific consequences of *Ube3a* loss toward the manifestation of pro-epileptogenic outcomes in AS, using mice in which maternal *Ube3a* was deleted selectively in either glutamatergic (*Ube3a*$^{fl/p+}$ *NEX-Cre*) or GABAergic (*Ube3a*$^{fl/p+}$ *Gad2-Cre*) neurons. Control and *Ube3a*$^{fl/p+}$ *NEX-Cre* mice exhibited similar flurothyl seizure susceptibility during the induction phase and at retest (Figure 2, A and B, and Supplemental Table 1). In contrast to what we observed in *Ube3a*$^{fl/p+}$ *NEX-Cre* mice, but consistent with our previous studies (12), we found that naive *Ube3a*$^{fl/p+}$ *Gad2-Cre* mice were highly susceptible to initial flurothyl exposure, exhibiting greatly reduced latency to seizure on the first trial of the kindling process and often succumbing to severe generalized seizures (Figure 2, C and D, trial 1). Given the high mortality of *Ube3a*$^{fl/p+}$ *Gad2-Cre* mice during 8-day flurothyl kindling (12), we opted to challenge *Ube3a*$^{fl/p+}$ *Gad2-Cre* mice with an abbreviated, 4-day flurothyl kindling paradigm. Control mice had significantly reduced seizure thresholds upon flurothyl retest (day 32) compared with day 1 in these experiments, demonstrating that the abbreviated kindling protocol was sufficient to promote epileptogenesis (Figure 2D; but see ref. 19). This effect was greatly exaggerated in *Ube3a*$^{fl/p+}$ *Gad2-Cre* mice, despite a flat kindling curve, possibly due to extremely low seizure threshold responses on day 1 (Figure 2, C and D, and Supplemental Table 1). Collectively, these findings reveal that loss of *Ube3a* selectively from GABAergic, but not glutamatergic, neurons enhances epileptogenic potential in a manner that is dissociable from reductions in acute (day 1) seizure threshold. These results also support excitation/inhibition (E/I) imbalance as a potential mechanism of epileptogenesis, as it is in ictogenesis (23), as presumably the positive E/I shift is much more robust in mice with GABAergic neuron–specific deletion than in mice with germline *Ube3a* deletion.

Though currently limited in the areas of safety and deliverability, the most promising AS treatment strategies to date are based on the replacement of neuronal UBE3A (14–17). AS mice with the capacity for conditional reinstatement of maternal *Ube3a* (*Ube3a*$^{STOP/p+}$ *Cre*$^{ERT+}$) provide a valuable preclinical model in which to evaluate the efficacy of this emerging therapeutic approach. These *Ube3a*-reinstatement mice have already been used to show that many AS phenotypes are impervious to rescue by reinstatement of *Ube3a* during adulthood (11). Similarly, we observed that enhanced epileptogenesis could not be rescued in adult *Ube3a*$^{STOP/p+}$ *Cre*$^{ERT+}$ mice through tamoxifen-induced (TAM-induced) reinstatement of *Ube3a* — either immediately after the completion (Figure 3A), or 2 weeks prior to the initiation (Figure 3B), of flurothyl kindling (Supplemental Figure 1, A and B). This suggested that the critical period for prevention of this pro-epileptogenic phenotype closes prior to adulthood. Accordingly, in subsequent experiments we initiated TAM injections in juvenile mice (at P21), well in advance of flurothyl kindling in adulthood. Juvenile restoration of *Ube3a* mitigated epileptogenesis in adult *Ube3a*$^{STOP/p+}$ *Cre*$^{ERT+}$ mice (Figure 3C), normalizing flurothyl retest responses to control levels without affecting the induction of kindling (Supplemental Figure 1C). Importantly, TAM treatment reinstated UBE3A to a similar level in both juvenile and adult mice (Supplemental Figure 2), suggesting that the selective antiepileptogenic effect of *Ube3a* reinstatement in juveniles is a function of early developmental intervention, and not an artifact of inefficient *Ube3a* reinstatement during adulthood. However, in our study, juvenile AS mice experienced a longer postintervention interval than adult AS mice, leaving open the possibility that a longer duration of *Ube3a* reinstatement could also be required for antiepileptogenic benefit. Thus, future studies are needed to determine whether some antiepileptogenic benefit can be realized in adult mice following a prolonged period of *Ube3a* reinstatement.

We found that flurothyl-kindled AS mice were highly susceptible to kainic acid (Figure 1G), which predominately triggers limbic seizures (22). Therefore, even though flurothyl kindling typically results in minor hippocampal pathology compared with models of temporal lobe epilepsy (24, 25), we suspected that hallmarks of hippocampal damage might be penetrant in flurothyl-kindled AS mice. We assayed 2 classic hippocampal pathological features: mossy fiber sprouting via zinc transporter 3 (ZnT3)

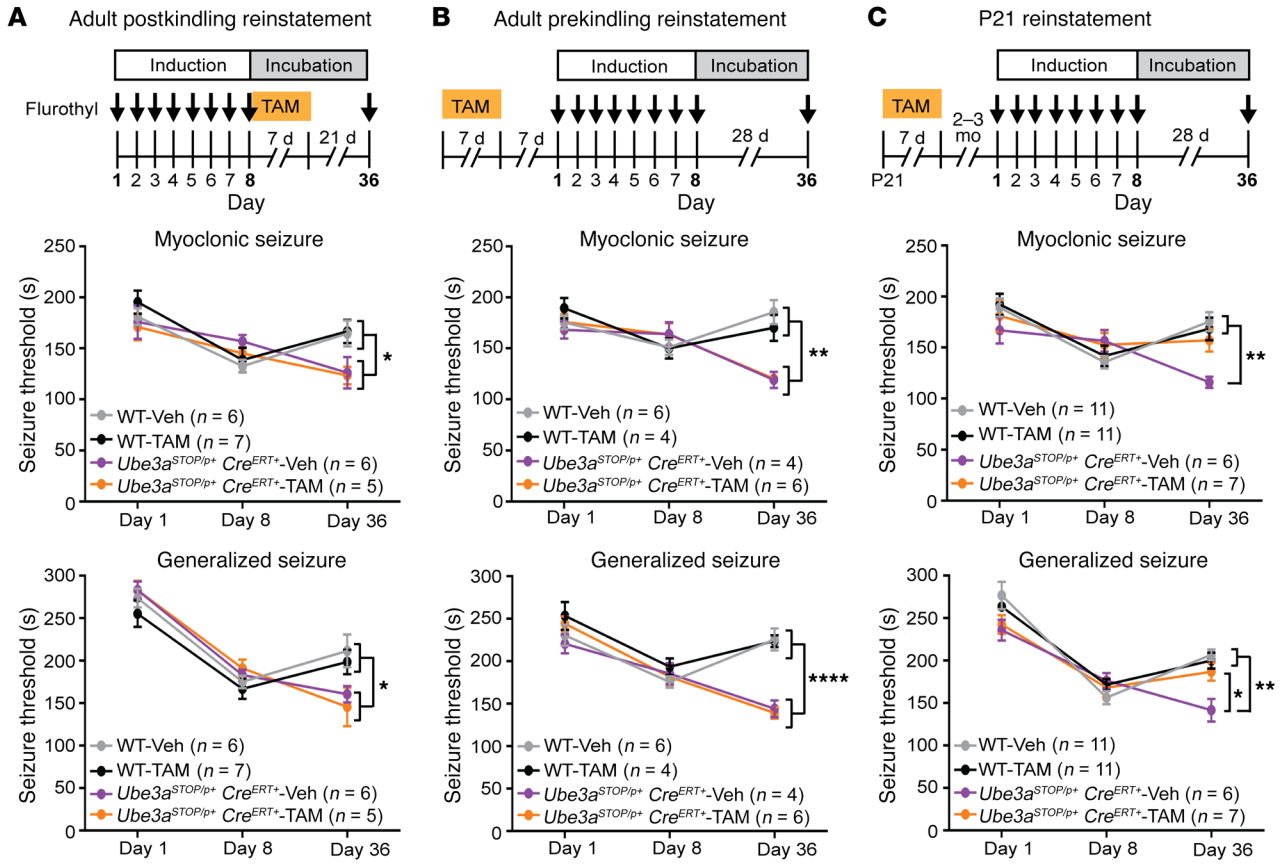

Figure 3. Prevention of exaggerated epileptogenesis in AS mice by reinstatement of *Ube3a* at P21, but not during adulthood. Myoclonic and generalized seizure responses to flurothyl kindling in *Ube3a*-reinstated mice (*Ube3a*$^{STOP/p+}$ *Cre*$^{ERT+}$-TAM) versus vehicle-treated (Veh) or tamoxifen-treated (TAM) controls (*Ube3a*$^{STOP/p+}$ *Cre*$^{ERT+}$-Veh, WT-Veh, and WT-TAM). We performed 7 days of once daily TAM (100 mg/kg, i.p.) or Veh injections to reinstate maternal *Ube3a* expression according to 3 different experimental schedules: (**A**) immediately following flurothyl kindling in adulthood; (**B**) 2 weeks prior to flurothyl kindling in adulthood; or (**C**) beginning at P21, with flurothyl kindling in adulthood. *$P < 0.05$, **$P < 0.01$, ****$P < 0.0001$ by 2-way ANOVA with Tukey's post hoc test. d, days; mo, months.

staining, and neuronal loss via NeuN staining. Neither was apparent in flurothyl-kindled mice, regardless of genotype (Figure 4A). We next questioned whether gross changes in the hippocampal extracellular matrix, perineuronal nets (PNNs) in particular, might associate with the exaggerated epileptogenesis phenotype in flurothyl-kindled AS model mice. PNNs are uniquely localized around specific neurons to regulate synapse stability and plasticity in the adult CNS (26), and have been associated with epileptic activity during early and late development (27–30). To examine a possible link between changes in PNNs and enhanced epileptogenesis in AS model mice, we labeled PNNs with biotinylated *Wisteria floribunda* agglutinin (WFA) in flurothyl-kindled mice before (Supplemental Figure 3), or 1 hour after (Figure 4, A and B), retest. We observed dramatically increased WFA staining selectively in the dentate gyrus granule cell layer and stratum moleculare of AS mice, regardless of sampling relative to retest (Figure 4, A and B, and Supplemental Figures 3 and 4). Vehicle-treated, flurothyl-kindled *Ube3a*$^{STOP/p+}$ *Cre*$^{ERT+}$ mice, which similarly lack maternal *Ube3a*, expressed this same PNN-related abnormality (Figure 4C). Importantly, juvenile reinstatement of *Ube3a* (*Ube3a*$^{STOP/p+}$ *Cre*$^{ERT+}$–TAM) normalized the PNN phenotype (Figure 4C), establishing that enhanced WFA staining in the dentate gyrus is a reliable anatomical correlate of enhanced epileptogenesis in flurothyl-kindled AS mice. Converging lines of evidence show that seizures can alter components of PNNs, but the specific proteins involved, and the direction and duration of changes may vary depending on a number of factors — the age of the animal, the seizure induction method, the brain region studied, and the time elapsed following seizure (27–30). Each of these factors, and hence the nature of the relationship between abnormal PNN deposition and epileptogenesis in AS model mice, remains to be rigorously investigated.

Seizures in AS patients usually begin in early childhood (4–6), but knowledge of the evolution of epilepsy in AS is scarce due to lack of rigorous retrospective or longitudinal studies. In this study, we used the flurothyl kindling and retest paradigm to demonstrate that AS model mice have a greatly enhanced capacity for epileptogenesis, which is rooted in the loss of *Ube3a* expression from GABAergic neurons. While additional studies will be required to resolve the developmental emergence of heightened epileptogenic susceptibility in AS mice — perhaps shedding light on the evolution of epilepsy in AS patients in the process — our results reveal that juvenile reinstatement of *Ube3a* normalizes epileptogenic potential later in adulthood. This suggests that *Ube3a* plays a

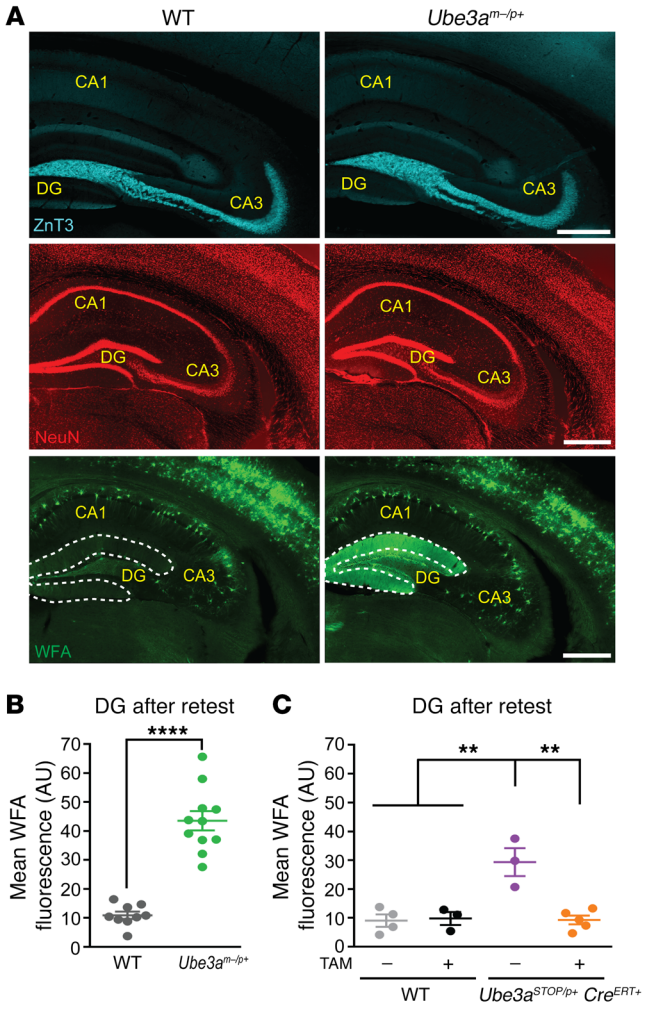

Figure 4. Increased deposition of PNNs in dentate gyrus of flurothyl-kindled AS mice. (**A**) Representative staining for ZnT3 (cyan) and costaining for NeuN (red) and WFA (green) in adjacent sections from WT and AS model mice euthanized 1 hour after flurothyl retest on day 36. Scale bars: 400 μm. DG, dentate gyrus. (**B** and **C**) Mean WFA fluorescence intensity (arbitrary units, AU) within dentate gyrus stratum moleculare. (**B**) WT (n = 9) versus AS (n = 11) model mice. ****$P < 0.0001$ by unpaired t test. (**C**) Control (Veh, n = 4; TAM, n = 3) and *Ube3a*$^{STOP/p+}$ *Cre*$^{ERT+}$ (Veh, n = 3; TAM, n = 5) mice treated with either Veh or TAM at P21. **$P < 0.01$ by 2-way ANOVA with Bonferroni's post hoc test.

critical role in developing GABAergic neural circuits with a robust capacity to withstand epileptogenic insults. In contrast, *Ube3a* provided little or no protection from epilepsy when added back to adult circuits, though it remains possible that a longer period following *Ube3a* reinstatement is required to guard against epileptogenic insults during adulthood.

Although it is difficult to equate postnatal stages of human and mouse development (31), our modeling experiments predict that the therapeutic window for treatment of epilepsy by *UBE3A* reinstatement extends well into childhood and perhaps as late as early adolescence. Comparable modeling studies imply that the prevention of other key AS phenotypes, including repetitive behavior and anxiety, requires *Ube3a* instatement much earlier during development (11). Dissimilar treatment windows for epilepsy compared with other AS phenotypes are not entirely unexpected; the onset of seizures in AS (average age 2.9 years; ref. 3) lags considerably behind the presentation of gross motor phenotypes and developmental delay during the first year of life (1). Presumably, for epilepsy to develop in AS, cellular and circuit-level pathologies gradually accumulate over a prolonged period of time.

The link between UBE3A loss and AS is unambiguous. *UBE3A* is located on chromosome 15, and is the only gene within the 15q11-q13 region that exhibits biased expression from the maternal allele. Accordingly, both deletions of maternal 15q11-q13 and loss-of-function point mutations of maternal *UBE3A* cause AS (32–34). Notably, in cases of AS caused by 15q11-q13 deletion, other genes, including a cluster of 3 $GABA_AR$ subunits, are also deleted (35, 36). This compound genetic insult presumably underlies increased penetrance and severity of seizure phenotypes (37), and may portend a commensurately limited efficacy of juvenile *UBE3A* reinstatement for treating epilepsy in 15q11-q13 deletion cases of AS relative to *UBE3A*-specific cases.

Collectively, our findings highlight the importance of carefully defining when *UBE3A* reinstatement will be efficacious in treating a range of AS phenotypes, which can differ significantly in terms of their onset and developmental trajectory. This knowledge will be invaluable in informing the design of upcoming clinical trials leveraging *UBE3A*-reinstatement therapies.

Methods

Detailed experimental methods are included with the supplemental materials. Male and female mice were used for experiments in equal genotypic ratios. Data are presented as mean ± SEM. Unpaired t tests (2-tailed) were used for single comparisons, and 2-way ANOVAs were used for multiple comparisons. $P < 0.05$ was considered significant.

Study approval. All animal procedures followed NIH guidelines and were approved by the IACUC at the University of North Carolina.

Author contributions

BG and KEC performed experiments. BG, KEC, and KAD analyzed the data. MCJ gave critical advice. MR and EPC managed the mouse colony and genotyping. BG, KEC, SMD, and BDP designed and coordinated the investigations. BG, KEC, MCJ, SMD, and BDP wrote the manuscript.

Acknowledgments

This work was supported by an American Epilepsy Society postdoctoral fellowship (to BG), the Intramural Research Program of the National Institute of Environmental Health Sciences and NIH grant ZIAES100221 (to SMD), National Institute of Neurological Disorders and Stroke grants R56NS097831 and R01NS085093, Eunice Kennedy Shriver National Institute of Child Health and Human Development grant R01HD093771, and the Angelman Syndrome Foundation (to BDP). We thank Klaus-Armin Nave and Ype Elgersma for providing *NEX-Cre* and *Ube3a*$^{m+/STOP}$ mice, respectively.

Address correspondence to: Benjamin D. Philpot, University of North Carolina, 115 Mason Farm Rd., Chapel Hill, North Carolina 27599-7545, USA. Phone: 919.966.0025; Email: bphilpot@med.unc.edu.

1. Williams CA, Driscoll DJ, Dagli AI. Clinical and genetic aspects of Angelman syndrome. *Genet Med*. 2010;12(7):385–395.
2. Buiting K, Williams C, Horsthemke B. Angelman syndrome — insights into a rare neurogenetic disorder. *Nat Rev Neurol*. 2016;12(10):584–593.
3. Thibert RL, et al. Epilepsy in Angelman syndrome: a questionnaire-based assessment of the natural history and current treatment options. *Epilepsia*. 2009;50(11):2369–2376.
4. Fiumara A, Pittalà A, Cocuzza M, Sorge G. Epilepsy in patients with Angelman syndrome. *Ital J Pediatr*. 2010;36:31.
5. Bakke KA, Howlin P, Retterstøl L, Kanavin ØJ, Heiberg A, Nærland T. Effect of epilepsy on autism symptoms in Angelman syndrome. *Mol Autism*. 2018;9:2.
6. Laan LA, et al. Evolution of epilepsy and EEG findings in Angelman syndrome. *Epilepsia*. 1997;38(2):195–199.
7. Born HA, et al. Strain-dependence of the Angelman syndrome phenotypes in Ube3a maternal deficiency mice. *Sci Rep*. 2017;7(1):8451.
8. Jiang YH, et al. Mutation of the Angelman ubiquitin ligase in mice causes increased cytoplasmic p53 and deficits of contextual learning and long-term potentiation. *Neuron*. 1998;21(4):799–811.
9. Mandel-Brehm C, Salogiannis J, Dhamne SC, Rotenberg A, Greenberg ME. Seizure-like activity in a juvenile Angelman syndrome mouse model is attenuated by reducing Arc expression. *Proc Natl Acad Sci U S A*. 2015;112(16):5129–5134.
10. Miura K, et al. Neurobehavioral and electroencephalographic abnormalities in Ube3a maternal-deficient mice. *Neurobiol Dis*. 2002;9(2):149–159.
11. Silva-Santos S, et al. Ube3a reinstatement identifies distinct developmental windows in a murine Angelman syndrome model. *J Clin Invest*. 2015;125(5):2069–2076.
12. Judson MC, et al. GABAergic neuron-specific loss of Ube3a causes Angelman syndrome-like EEG abnormalities and enhances seizure susceptibility. *Neuron*. 2016;90(1):56–69.
13. Sidorov MS, et al. Delta rhythmicity is a reliable EEG biomarker in Angelman syndrome: a parallel mouse and human analysis. *J Neurodev Disord*. 2017;9:17.
14. Daily JL, et al. Adeno-associated virus-mediated rescue of the cognitive defects in a mouse model for Angelman syndrome. *PLoS ONE*. 2011;6(12):e27221.
15. Huang HS, et al. Topoisomerase inhibitors unsilence the dormant allele of Ube3a in neurons. *Nature*. 2011;481(7380):185–189.
16. Meng L, Ward AJ, Chun S, Bennett CF, Beaudet AL, Rigo F. Towards a therapy for Angelman syndrome by targeting a long non-coding RNA. *Nature*. 2015;518(7539):409–412.
17. Bailus BJ, et al. Protein delivery of an artificial transcription factor restores widespread Ube3a expression in an Angelman syndrome mouse brain. *Mol Ther*. 2016;24(3):548–555.
18. Kadiyala SB, et al. Eight flurothyl-induced generalized seizures lead to the rapid evolution of spontaneous seizures in mice: a model of epileptogenesis with seizure remission. *J Neurosci*. 2016;36(28):7485–7496.
19. Samoriski GM, Applegate CD. Repeated generalized seizures induce time-dependent changes in the behavioral seizure response independent of continued seizure induction. *J Neurosci*. 1997;17(14):5581–5590.
20. Ben-Ari Y, Crepel V, Represa A. Seizures beget seizures in temporal lobe epilepsies: the boomerang effects of newly formed aberrant kainatergic synapses. *Epilepsy Curr*. 2008;8(3):68–72.
21. Tse K, Puttachary S, Beamer E, Sills GJ, Thippeswamy T. Advantages of repeated low dose against single high dose of kainate in C57BL/6J mouse model of status epilepticus: behavioral and electroencephalographic studies. *PLoS One*. 2014;9(5):e96622.
22. Ben-Ari Y. Limbic seizure and brain damage produced by kainic acid: mechanisms and relevance to human temporal lobe epilepsy. *Neuroscience*. 1985;14(2):375–403.
23. Fritschy JM. Epilepsy, E/I balance and GABA(A) receptor plasticity. *Front Mol Neurosci*. 2008;1:5.
24. Ferland RJ, Gross RA, Applegate CD. Increased mitotic activity in the dentate gyrus of the hippocampus of adult C57BL/6J mice exposed to the flurothyl kindling model of epileptogenesis. *Neuroscience*. 2002;115(3):669–683.
25. Kadiyala SB, et al. Spatiotemporal differences in the c-fos pathway between C57BL/6J and DBA/2J mice following flurothyl-induced seizures: A dissociation of hippocampal Fos from seizure activity. *Epilepsy Res*. 2015;109:183–196.
26. Sorg BA, et al. Casting a wide net: role of perineuronal nets in neural plasticity. *J Neurosci*. 2016;36(45):11459–11468.
27. McRae PA, Baranov E, Rogers SL, Porter BE. Persistent decrease in multiple components of the perineuronal net following status epilepticus. *Eur J Neurosci*. 2012;36(11):3471–3482.
28. McRae PA, Baranov E, Sarode S, Brooks-Kayal AR, Porter BE. Aggrecan expression, a component of the inhibitory interneuron perineuronal net, is altered following an early-life seizure. *Neurobiol Dis*. 2010;39(3):439–448.
29. McRae PA, Porter BE. The perineuronal net component of the extracellular matrix in plasticity and epilepsy. *Neurochem Int*. 2012;61(7):963–972.
30. Rankin-Gee EK, McRae PA, Baranov E, Rogers S, Wandrey L, Porter BE. Perineuronal net degradation in epilepsy. *Epilepsia*. 2015;56(7):1124–1133.
31. Workman AD, Charvet CJ, Clancy B, Darlington RB, Finlay BL. Modeling transformations of neurodevelopmental sequences across mammalian species. *J Neurosci*. 2013;33(17):7368–7383.
32. Kishino T, Lalande M, Wagstaff J. UBE3A/E6-AP mutations cause Angelman syndrome. *Nat Genet*. 1997;15(1):70–73.
33. Matsuura T, et al. De novo truncating mutations in E6-AP ubiquitin-protein ligase gene (UBE3A) in Angelman syndrome. *Nat Genet*. 1997;15(1):74–77.
34. Sutcliffe JS, et al. The E6-Ap ubiquitin-protein ligase (UBE3A) gene is localized within a narrowed Angelman syndrome critical region. *Genome Res*. 1997;7(4):368–377.
35. Saitoh S, et al. Familial Angelman syndrome caused by imprinted submicroscopic deletion encompassing GABAA receptor beta 3-subunit gene. *Lancet*. 1992;339(8789):366–367.
36. Wagstaff J, et al. Localization of the gene encoding the GABAA receptor beta 3 subunit to the Angelman/Prader-Willi region of human chromosome 15. *Am J Hum Genet*. 1991;49(2):330–337.
37. DeLorey TM, et al. Mice lacking the β3 subunit of the GABAA receptor have the epilepsy phenotype and many of the behavioral characteristics of Angelman syndrome. *J Neurosci*. 1998;18(20):8505–8514.